On the Accuracy of Theoretically and Experimentally Determined Electron Densities of Polar Bonds

Julian Henn,[†] Dagmar Ilge,[‡] Dirk Leusser,[‡] Dietmar Stalke,[‡] and Bernd Engels*,[†]

Institut für Organische Chemie and Institut für Anorganische Chemie, Universität Würzburg, Am Hubland, D-97074 Würzburg, Germany

Received: May 19, 2004; In Final Form: July 16, 2004

In the present study, we employ a set of different sulfur−nitrogen compounds, which contains eight different SN bonds of varying polarity, to study descrepancies between experimentally and theoretically derived electron densities characterized by their topological properties at the bond critical point according to Bader's quantum theory of atoms in molecules approach. First, the convergency of the computationally obtained parameters with respect to the theoretical approach (flexibility of the basis sets, method of computation, influence of substituents) is presented. A comparison with the experiment is performed by a direct comparison of the theoretical and experimental counterparts and by an investigation into what extent the various data sets exhibit relationships to the nature of the bonds. This approach allows testing of the self-consistency of the theoretical and experimental data, respectively. Finally, the outcomes of the atoms-in-molecules approach is compared with results obtained from the natural bond orbital approach and natural resonance theory.

I. Introduction

The electron density distribution (ED) $\rho(\mathbf{r})$ represents a fundamental quantity which determines all chemical and physical phenomena, for example, intra- and intermolecular forces, molecular geometry, electrostatic potential, and chemical bonding.[1−7] It is the underlying quantity in density functional theory (DFT)[8,9] and is also readily available from wavefunction-based approaches. However, despite its importance, the density is discussed less frequently in theoretical investigations, although it represents a physical observable phenomenon. It is measurable, for instance, by high-resolution X-ray diffraction experiments.[2,3,6,10]

The development of area detectors, often in combination with the usage of very bright third-generation synchrotron sources, has opened new horizons for the use of X-ray diffraction in the experimental determination of the electron density, because the time necessary for data acquisition shrinks considerably.[11−14] A very enticing intrinsic feature of an experimentally determined electron density is the fact that it includes all many-body effects (e.g., electron correlation, relativistic effects, influence of the environment). This renders it an ideal tool to analyze the shortcomings of theoretical approaches, which, because of the complexity of the systems, have to neglect or approximate parts of the interactions. The quantum theory of atoms in molecules (QTAIM) approach developed by Bader and co-workers,[1] in which the topological properties of the electron density are interpreted, represents the most straightforward comparison between experimental results and theory, but other approaches are also under development.[15−19]

An even more attractive goal of high-resolution X-ray diffraction experiments represents their ability to describe large systems such as biological macromolecules which are still too large for a reliable theoretical description.[20,21] One direction of the ongoing research in this area is the attempt to construct such systems from the overlay of the density of smaller subunits (e.g., single amino acids).[14,22−26] It is clear that a success would open not only the possibility to describe the electronic properties of biological macromolecules but also the determination of the bonding strength[14,22−27] (e.g., within an enzyme inhibitor complex, which is essentially for the development of agents against infectious diseases).

The conditio sine qua non for all of these goals is that the experimental electron density is not biased by assumptions or shortcomings of the procedures necessary to get it from the measured quantities (i.e., Bragg reflections and their intensities). Indeed, various recent studies indicate that the Hansen−Coppens multipole formalism,[2,28] which is mostly used to derive the ED from the experimental diffraction data, introduces such a bias.[29−31] It results because the basis sets used to describe the electron density distribution seem to be not flexible enough to reflect the subtle details of electron densities in polar bonds. As discussed by the authors, this seems to be at least partly the reason for the differences found between experimentally and theoretically determined topological properties at the bond critical point (BCP). As shown in many investigations, such differences appear particularly for polar bonds. These exhibit nonsymmetric interatomic densities and Laplacian distributions.[2,6,14,22−27,32] For nonpolar bonds experimentally and theoretically derived, bond topological values are in excellent agreement.[6,33,34] It is also found that in most cases experiment and theory agree qualitatively; for example, in the number of bond critical points or the number of valence-shell charge concentrations (VSCC).[6,14,35,36] A bias could also be introduced in specific cases where two or more parameter sets of the multipole model exist, which are of similar quality in residual density and statistical quality. Such nonuniqueness was demonstrated (e.g., by Peres et al).[37]

However, the disagreement in the absolute numbers of the topological properties could also result from shortcomings in the theoretical description. On one hand, the influence of the crystal environment on the molecule, which is often not included in the theoretical description, seems to be too small to explain the descrepancies between experimental results and theory, as already shown.[38−40] On the other hand, the Hartree−Fock

* Corresponding author. E-mail: bernd@chemie.uni-wuerzburg.de.
[†] Institut für Organische Chemie.
[‡] Institut für Anorganische Chemie.

10.1021/jp047840a CCC: $27.50
Published on Web 10/01/2004

approach, for example, is well-known for predicting bonds which are too polar (e.g., the inclusion of correlation effects is important to obtain reliable electron densities[41−43]). The MP2 approach already predicts topological parameters in close agreement with even more sophisticated approaches such as MP4 or QCISD.[22,44] A similar behavior is found for DFT if hybrid functionals are used, while results obtained with gradient corrected functionals deviate more strongly.[22,44] Also, the influence of the flexibility of the AO basis sets employed in the computations were tested to some extent. An influence is seen, but it is too small to explain the deviations between experimental results and theory. However, with the exception of very small model systems, the tested basis sets do not exceed triple-ζ quality.[22,44]

Besides the comparison of absolute numbers, an investigation of the correlations between the topological parameters and the bonding type can also reveal important information about the quality of the results. Such correlations are expected and are used in many investigations.[2,3,6,34,45,35] One example is the position of the bond critical point, which, as shown by Cremer and Kraka, correlates with the polarity of the bond.[45] From Bader's QTAIM approach,[1] correlations are also expected for the density, its second derivative along the bond path (λ_3), and the bond ellipticity ϵ, which is obtained from the second derivatives of the density perpendicular to the bond paths ($\epsilon = \lambda_1/\lambda_2 - 1$). The latter also gives information about the delocalization within a molecule.[35,46] Consequently, results which do not reveal such correlations can be expected to be biased to some extent. This is especially true if correlations are found for the less sensitive parameters (e.g., density) but are missing for more sensitive ones (e.g., Laplacian values). For the homoatomic CC bonds of C_{60} fullerene derivatives, Wagner et al.[34] found the expected relationships between the density at the BCP and the bond distances and between the Laplacian at the BCP and the bond distances. This shows that high-resolution synchrotron diffraction experiments are able to give very accurate descriptions of such covalent nonpolar bonds. However, whether this also holds true for polar bonds is unclear.

In a previous paper,[36] we employed theoretically and experimentally determined electron density distributions of methyl-(diimido)sulfinic acid H(N*t*Bu)$_2$SMe (**1**), methylene−bis-(triimido)sulfonic acid H$_2$C[S(N*t*Bu)$_2$H(N*t*Bu)]$_2$ (**2**), sulfurdiimide S(N*t*Bu)$_2$ (**3**), and sulfurtriimide S(N*t*Bu)$_3$ (**4**) (see Figure 1) to elucidate the characters of the different SN bonds. For this instance, we applied the topological theory of molecular structure of the QTAIM approach for the interpretation of the (theoretically and experimentally determined) electron densities and compared the results to the NBO (natural bond orbital)/NRT (natural resonance theory) description, which is based on the wavefunctions obtained from the computations. Experimental and theoretical values were found to be in good agreement regarding the overall picture of the nature of the bonds as obtained from the numbers, shapes, and positions of the VSCCs. Excellent agreement was obtained for the qualitative spatial Laplacian distributions and the reactive surfaces; however, the quantitative values at the BCP differed considerably.

Because this set of model systems contains many bonds of varying polarity, it is ideally suited to study discrepancies between theory and experiment. For this, we first investigate the convergency of the theoretical values with respect to the method of computations, employing different DFT approaches and, also, the MP2 method. To study the influence of the basis set, we go up to basis sets the size of cc-pV5Z. The computed values are compared to their experimental counterparts, and to shed some light onto the self-consistency of the data, we also investigate possible relationships between the density and its Laplacian at the BCP with the bond distances. Additionally, the convergency of the NBO/NRT approach[47] with repect to the method of computation is tested, and its predictions about the bond characters are compared to those obtained from the topological parameters of the QTAIM approach.

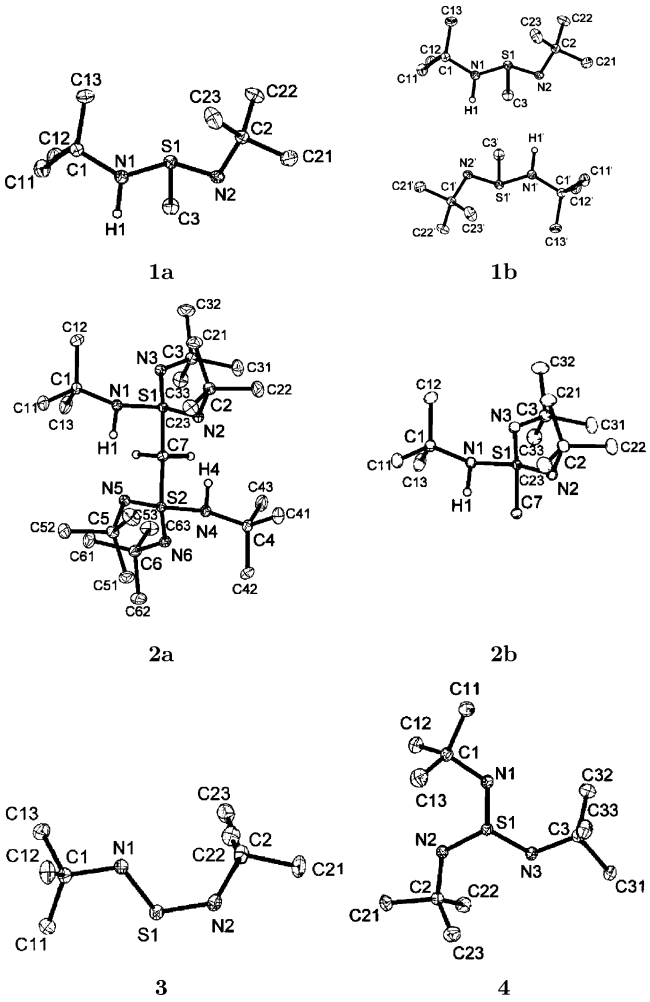

Figure 1. The connectivity of the molecules under consideration: The sulfinic acid, **1a**; the sulfinic acid as a dimer, as in the solid state, **1b**; the sulfonic acid, **2a**; the S(NHR)(NR)$_2$CH$_3$, **2b**; the diimide, **3**; and the triimide, **4**.

II. Computational Methods

Gas-phase structures of the model compounds were optimized for different substituents R = H, Me, and *t*Bu, respectively, employing a great variety of theoretical methods. Stationary points were checked by frequency calculations. All calculations were performed with the *Gaussian 98* package.[48] The subsequent topological analyses were performed with the *AIM2000* package,[49] while the NBO/NRT analyses were performed with the *NBO 4.M* package.[47] As far as bond orders are discussed outside NBO/NRT theory, we are referring to bond orders according to Cioslowski.[50] This approach divides the total number of electrons in atomic and diatomic contributions by means of evaluating the atomic overlap matrix under consideration of the atomic boundaries and yields positive, purely covalent bond orders.

TABLE 1: Bond Topological Properties at the BCP of the Formal S1═N2 Double Bond in 1a; R = Me[a]

	d	ρ	$\nabla^2\rho$	λ_1	λ_2	λ_3	ϵ	*d*(N)	*d*(S)	*d*(N)/*d*(S)	$\lvert\lambda_1\rvert/\lambda_3$
					B3PW91						
6-31G(d)	1.55	1.76	8.36	−10.01	−7.14	25.52	0.40	0.96	0.60	1.61	0.39
6-31G(d,p)	1.55	1.76	8.33	−10.02	−7.14	25.5	0.40	0.96	0.60	1.61	0.39
6-31G(2d,p)	1.54	1.83	−5.22	−11.25	−8.27	14.30	0.36	0.92	0.62	1.48	0.79
6-31G(3d,p)	1.53	1.86	1.46	−11.65	−8.57	21.68	0.36	0.92	0.61	1.52	0.54
6-31+G(d)	1.55	1.76	8.02	−10.01	−7.15	25.18	0.4	0.96	0.60	1.60	0.40
6-31+G(d,p)	1.55	1.76	7.89	−10.00	−7.15	25.04	0.40	0.96	0.60	1.60	0.40
6-311G(d,p)	1.54	1.80	6.14	−10.31	−7.51	23.96	0.37	0.95	0.60	1.58	0.43
6-311G(2d,p)	1.53	1.86	−6.68	−11.45	−8.44	13.21	0.36	0.91	0.63	1.46	0.87
6-311G(3d,p)	1.53	1.87	0.45	−11.70	−8.61	20.76	0.36	0.92	0.61	1.50	0.56
cc-pVDZ	1.56	1.67	9.25	−8.85	−6.46	24.58	0.37	0.96	0.60	1.60	0.36
cc-pVTZ	1.54	1.86	3.65	−11.02	−7.77	22.43	0.42	0.94	0.60	1.56	0.49
					B3LYP						
6-311G(d,p)	1.55	1.79	4.62	−10.31	−7.50	22.44	0.37	0.95	0.60	1.58	0.46
					MP2						
6-31G(d)	1.57	1.67	4.40	−9.09	−6.46	19.94	0.41	0.97	0.61	1.61	0.46
6-31G(2d,p)	1.57	1.71	−7.82	−9.98	−7.42	9.58	0.34	0.93	0.64	1.44	1.02
					Experimental						
	1.53	2.24	−9.38	−12.58	−11.73	14.92	0.07	0.74	0.79	0.94	0.84

[a] The geometry was optimized at the indicated level of theory. Distances are given in Å, densities are given in e/Å^3, and second derivatives are given in e/Å^5.

TABLE 2: Bond Topological Properties at the BCP of the Formal S1—N1 Single Bond in 1a; R = Me[a]

	d	ρ	$\nabla^2\rho$	λ_1	λ_2	λ_3	ϵ	*d*(N)	*d*(S)	*d*(N)/*d*(S)	$\lvert\lambda_1\rvert/\lambda_3$
					B3PW91						
6-31G(d,p)	1.75	1.31	−8.46	−6.94	−6.34	4.81	0.09	0.98	0.77	1.27	1.44
6-31G(2d,p)	1.74	1.30	−6.35	−7.10	−6.45	7.20	0.10	0.94	0.80	1.18	0.99
6-31G(3d,p)	1.73	1.36	−8.49	−7.32	−6.65	5.49.	0.10	0.98	0.75	1.31	1.33
6-311G(d,p)	1.75	1.32	−8.58	−7.32	−6.71	5.45	0.09	0.95	0.80	1.19	1.34
6-311G(2d,p)	1.74	1.31	−6.67	−7.37	−6.64	7.34	0.11	0.92	0.82	1.13	1.00
6-311G(3d,p)	1.73	1.36	−8.85	−7.56	−6.86	5.56	0.10	0.95	0.77	1.23	1.36
cc-pVDZ	1.77	1.24	−6.25	−6.06	−5.55	5.36	0.09	0.99	0.78	1.28	1.13
cc-pVTZ	1.73	1.38	−9.95	−7.84	−6.98	4.88	0.12	0.94	0.79	1.20	1.61
					B3LYP						
6-311G(d,p)	1.75	1.30	−8.40	−7.32	−6.74	5.67	0.09	0.95	0.80	1.18	1.29
					Experimental						
	1.68	1.76	−7.95	−10.26	−9.66	11.97	0.06	0.83	0.85	0.98	0.86

[a] The geometry was optimized on the indicated level of theory. Distances are given in Å, densities are given in e/Å^3, and second derivatives are given in e/Å^5.

TABLE 3: Bond Topological Properties at the BCP of the S1—C3 Bond in 1a; R = Me[a]

	d	ρ	$\nabla^2\rho$	λ_1	λ_2	λ_3	ϵ	*d*(S)	*d*(C)	*d*(S)/*d*(C)	$\lvert\lambda_1\rvert/\lambda_3$
					B3PW91						
6-31G(d,p)	1.81	1.30	−8.65	−7.42	−7.02	5.79	0.06	0.96	0.85	1.13	1.28
6-31G(2d,p)	1.80	1.27	−6.69	−6.90	−6.50	6.71	0.06	0.95	0.85	1.12	1.03
6-31G(3d,p)	1.80	1.33	−8.98	−7.56	−7.12	5.69	0.06	0.95	0.85	1.12	1.33
6-311G(d,p)	1.81	1.29	−8.09	−7.52	−7.11	6.55	0.06	0.97	0.84	1.15	1.15
6-311G(2d,p)	1.80	1.25	−6.08	−7.01	−6.60	7.53	0.06	0.95	0.85	1.12	0.93
6-311G(3d,p)	1.80	1.32	−8.30	−7.62	−7.19	6.51	0.06	0.95	0.84	1.13	1.17
cc-pVDZ	1.81	1.29	−9.19	−6.99	−6.57	4.38	0.06	0.96	0.85	1.13	1.60
cc-pVTZ	1.80	1.32	−8.32	−7.82	−7.34	6.84	0.06	0.95	0.85	1.12	1.14
					B3LYP						
6-311G(d,p)	1.82	1.27	−7.69	−7.44	−7.06	6.81	0.05	0.97	0.85	1.14	1.09
					Experimental						
	1.79	1.54	−8.70	−9.18	−8.72	9.20	0.05	0.99	0.80	1.24	1.05

[a] The geometry was optimized at the indicated level of theory. Distances are given in Å, densities are given in e/Å^3, and second derivatives are given in e/Å^5.

III. Results and Discussion

A. Investigation of the Method Dependency of Bond Topological QTAIM Properties and Comparison with Experimental Results. Tables 1−3 summarize the computed bond topological properties of some typical bonds of our set of model systems as a function of the method of computation. For a formal SN double bond, we picked S1═N2 of compound **1a** (R = Me, Table 1), while S1—N1 of the same compound was chosen for a formal SN single bond (Table 2). As a typical example for the less polar SC and NC bonds to a methyl (or butyl) group, we give the bond topological properties of the S—C bond of the same compound (Table 3). The tables contain the computed bond distance of the given bond, denoted as *d*, the density at the BCP, ρ, the Laplacian at the BCP, $\nabla^2\rho$, the decomposition of the Laplacian into its three Eigenvalues $\nabla^2\rho = \lambda_1 + \lambda_2 + \lambda_3$, the ellipticity $\epsilon = \lambda_1/\lambda_2 - 1$, and the respective distances of the BCP to atom A, *d*(A) and to the other atom, *d*(B). Additionally, the ratio *d*(A)/*d*(B) is shown. The ratio $\lvert\lambda_1\rvert/\lambda_3$, which is expected to be smaller than 1 in ionic bonding modes,[1] is also given. At the BCP, the negative Eigenvalues, λ_1 and λ_2, describe the local charge concentrations in a plane with normal vector in the direction of the interatomic

line; λ_1 is defined to be greater than λ_2, such that the ratio $\lambda_1(\mathbf{r})/\lambda_2(\mathbf{r})$ always exceeds 1. A large value of this ratio indicates π-like electron distribution. The positive Eigenvalue λ_3 describes the local charge depletion due to monotonic decreasing electron densities from the nuclei to the BCP. Like the electron density, all of its derivatives, including $\nabla^2\rho$, λ_1, λ_2, and λ_3, are functions of the spatial variable **r**. Thus, the values of, for example, the ellipticity ϵ, are sensitive to the position of the BCP.[51] We investigated the convergency of the various properties with respect to the flexibility of the basis set and tested their sensitivities with respect to the functional (using Becke's B3 exchange functional[52,53] in combination with the PW91[54] and the LYP[55] correlation functionals, respectively) and the MP2 method. As expected from other DFT studies[4,6,22,23,27,42−44] a 6-311G(2d,p)[56−60] or a cc-pVTZ[61−66] basis set seems to be sufficient to obtain bond distances converged to about 0.01 Å for the strong formal double bond. For smaller AO basis sets, variations up to 0.04 Å for the present model systems were obtained. Within the QTAIM theory, the properties at the BCP play a crucial role such that its position can be expected to represent a sensitive parameter. As shown in Tables 1−3 for the present model systems, the positions of the BCPs vary only slightly as a function of the theoretical method (∼3%). For the formal S1═N2 double bond of compound **1a**, its distance from the nitrogen center changes from 0.95 to 0.91 to 0.92 Å for the series 6-311G(d,p), 6-311G(2d,p), and 6-311G(3d,p), and also, the flexibility of the sp part (6-31G sets vs 6-311G sets) has a small influence. If the PW91 correlation functional is replaced by the LYP functional, only minor differences are found. The differences between the MP2 and DFT approaches are somewhat larger, as discussed elsewhere.[22,44] For the chosen formal S−N single bond (Table 2), the position of the BCP varies more strongly as a function of the theoretical approach in comparison to the formal double bonds. For the S−C bond (Table 3), the variation is less. It is interesting to note that, going from the S1═N2 double bond (Table 1) to the single bond (Table 2), the distance between the BCP and the nitrogen center does not change much (≤0.06 Å), while the distance between the BCP and the sulfur center increases by approximately 0.16 Å.

The densities ρ's at the BCP as well vary only slightly with the method of computations. For formal double bonds as shown in the example of the S1═N2 bond of compound **1a** within the series 6-311G(d,p), 6-311G(2d,p), and 6-311G(3d,p), the values change from 1.80 to 1.87 e/Å^3. Please note that the value computed with the cc-pVDZ basis set is smaller than that obtained with the 6-31G(d,p) basis set, while both cc-pVTZ and 6-311G(2d,p) give similar values. In general, the MP2 approach predicts somewhat smaller values than DFT, which could result from the slightly enlarged bond distances.

Although the position of the BCP and the density at the BCP are not very sensitive with respect to the basis set size and method of computation, the Eigenvalues of the Laplacian of the density λ_i, $i = 1, 2, 3$, at the BCP vary considerably for S1═N2 of compound **1a** (R = Me, Table 1), which was picked as a typical formal SN double bond. As shown in Table 1, especially, λ_3 changes as a function of the flexibility of the basis set (e.g., with increasing numbers of d functions). Please note that the λ_3 values obtained with the standard *GAUSSIAN* (2d,p) set of polarization functions deviate strongly from the 1d and 3d results, and so, the (2d,p) results have to be regarded as outliers. Smaller variations are found for λ_1 and λ_2. As a consequence, also, the computed values for ϵ, which according to the QTAIM theory of Bader are used to obtain information about the bond order, decrease only from 0.40 to 0.36 if the basis set flexibility is increased. For λ_1 and λ_2, the (1d,p), (2d,p), (3d,p) series of polarization functions show smooth behavior. As a consequence of the strong change in λ_3, the Laplacian $\nabla^2\rho$ even changes its sign if the number of polarization functions is increased [6-311G(d,p) + 6.14 e/Å^5, 6-311G(2d,p) − 6.68 e/Å^5, 6-311G(3d,p) + 0.45 e/Å^5]. Even if the (2d,p) basis set is considered as an outlier, $\nabla^2\rho$ still drops appreciably if the number of d polarization functions is increased.

For comparison, Table 1 also gives the experimental values obtained from a high-resolution X-ray study.[36] As already discussed in this paper for the present set of model compounds, experiment and theory agree qualitatively very well but disagree in the absolute values. As shown in Table 1, all experimental values are obviously outside the range spanned by the theoretical data. The experimentally determined density at the BCP is considerably higher (∼25%) than its theoretical counterpart. For the formal SN double bonds, the experiment determines λ_1 and λ_2 to be almost equal, while a profound difference is predicted by all computations (see Tables 1 and 8). As a consequence, also, the experimentally and theoretically derived ϵ values disagree. Surprisingly, the experimental value of λ_3 is close to the prediction obtained with the (2d,p) set of polarization functions, which was identified as an outlier in theory. Finally, the positions of the BCPs also differ. For formal double bonds, the experimental values are approximately in the middle of the bond, while theory predicts a position much closer to the sulfur center.

Before we come to a more detailed discussion of these differences, we will first discuss the other types of bonds. For the selected typical formal SN single bonds (Table 2), the deviation between experimentally and theoretically determined bond distances is somewhat larger than for the double bonds (still 0.05 Å for the 6-311G(3d,p) basis set), because the former possesses flatter potentials than the formal double bonds. For the formal SN single bonds, the absolute value of λ_3 and, also, its variations are considerably smaller, compared to the formal SN double bonds. Also, as a consequence, the Laplacian $\nabla^2\rho$ changes to a smaller extent. This also holds true for the other density-related properties, such that the agreement between theory and experiment is, in general, better. One example is the position of the BCP. Please note that in comparison to the formal SN double bond (Table 1) better agreement results, because the theoretical [d(N)/d(S)] values change considerably from about 1.5−1.6 for the formal double bond to approximately 1.2 for the formal single bond. The experimentally obtained values for both types of bonds are virtually identical. Another example for a better agreement is ϵ. However, while both theory and experiment find λ_1 and λ_2 to be very similar for the formal single bonds, they disagree in the absolute values.

The computed values of λ_3 are smaller than their experimental counterparts for the formal single bonds (Tables 2 and 3). The smaller theoretical absolute values of λ_1 and λ_2 and the lower theoretical value of λ_3 cancel each other, so that theory and experiment agree with respect to the Laplacian. It is interesting that, on the basis of ϵ, there is no difference between formal single and double bonds in the experimental values.

The topological properties of the S−C bond of compound **1a**, which was selected as a typical bond for the less polar S−C bonding, is given in Table 3. For this type of bond, the variations within the theoretical results are much smaller than for the previous two types. In accordance with the former results, the computations again find the (2d,p) to represent an outlier. In addition to the reduced dependency on the method of calculation, the agreement between theory and experiment is much better

TABLE 4: Bond Topological Properties at the BCP of the S1═N1 Bond in 3 (R = H), Calculated with the B3PW91 Functional and Indicated Basis Sets[a]

basis set	ρ	$\nabla^2\rho$	$-\lambda_1$	$-\lambda_2$	λ_3	d(N)/d(S)
cc-pVDZ	1.66	8.66	8.577	6.569	23.802	1.60
cc-pVTZ	1.83	2.62	10.738	7.897	21.260	1.56
cc-pVQZ	1.91	0.15	12.384	9.157	21.700	1.55
cc-pV5Z	1.92	0.83	12.847	9.603	23.280	1.54
6-311G	1.62	−0.09	7.709	6.825	14.442	1.44
6-311G(d)	1.79	5.92	10.073	7.685	23.682	1.59
6-311G(d,p)	1.79	5.68	10.143	7.741	23.561	1.59
6-311G(2d,p)	1.85	−7.19	11.314	8.596	12.717	1.46
6-311G(3d,p)	1.86	−0.46	11.524	8.784	19.319	1.51

[a] The geometry was optimized on the indicated level of theory. Distances are given in Å, densities are given in e/Å^3, and second derivatives are given in e/Å^5.

for all derivatives of the density at the BCP. For the density itself, theory again predicts much lower values. Both theory and experiment locate the BCP closer to the carbon center.

To investigate the dependency of the λ_i values as a function of the basis set flexibility in more detail, we computed the topological QTAIM properties of the formal S1═N1 double bond of compound **3** (R = H) for the cc basis set series (Table 4). The SN formal double bonds were found to be problematic with respect to λ_3. Table 4 also gives the values obtained with the 6-311G basis set enlarged with an increasing number of d functions. With respect to the Laplacian, $\nabla^2\rho$, this bond is found to behave similarly to the S1═N2 bond of compound **1a** described in Table 1 (i.e., $\nabla^2\rho$ gets initially considerablely smaller with increasing basis set size). For the cc series, both λ_1 and λ_2 show convergency with respect to the basis set size. For λ_3, however, a change of about 10% is still found if the cc-pVQZ basis set is compared to the cc-pV5Z basis set. The influence of basis set size on the Laplacian $\nabla^2\rho$ at the BCP is somewhat smaller, because the changes in the λ_i values compensate to some extent. Table 4 also underlines the fact that results obtained with the standard 2d set of polarization functions of the Pople basis set deviate considerably from those obtained with other basis sets.

A first hint to the reasons for the dependence of the λ_3 values on the method of calculation stems from the [d(N)/d(S)] values. For both formal SN double bonds, S1═N2 of compound **1** (R = Me, Table 1) and S1═N1 of compound **3** (Table 4), values around 1.5 were computed (i.e., the BCP is located considerably closer to the sulfur center then to the nitrogen center). Similar values are found for all formal SN double bonds of the present model systems. For the S1−N1 bond in **1a** (Table 2), values around 1.2 were computed, while values of approximately 1.1 are obtained for the S−C bond in **1a**. These values are typical for the formal single S−N and S−C bonds. This shows that, when going from formal SN double bonds to formal single bonds, the BCP moves away from the sulfur center more into the middle of the bonds. The consequence for the density and its Laplacians can be taken from Figure 2 , in which the density and the λ_i values are plotted along the S1═N1 bond path in compound **4** (R = *t*Bu). For this computation, the experimental geometry was used. For this formal SN double bond, the BCP is located in a region, where λ_1 and λ_2 vary slowly, while λ_3 abruptly changes toward very large positive values, a situation that can be properly described with the BCP lying in the rampant edge of the Laplacian. A tiny displacement of the BCP to the right would change the sign of the Laplacian, while a tiny displacement to the left would lead to a strong increase of the Laplacian. Consequently, already the small changes in the position of the BCP discussed already lead to large changes in the λ_3 value and the Laplacian. This explains the strange

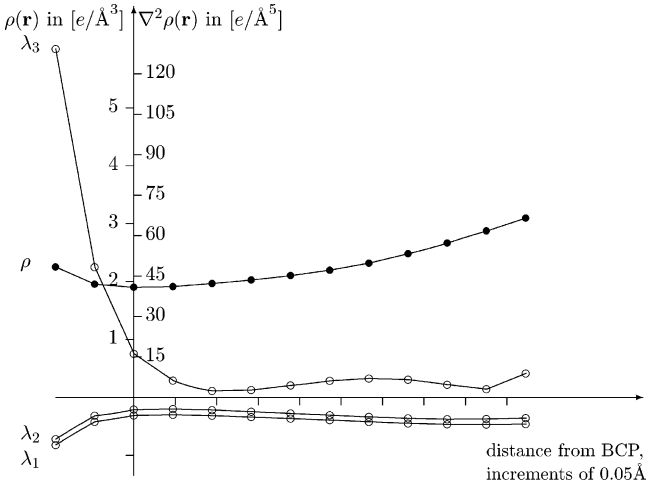

Figure 2. Eigenvalues λ_i (empty circles, ○) and the density along the bond path (filled circles, ●) in **4**, R = *t*Bu, calculated at the B3PW91/6-311++G(d,p) level of theory with fixed experimental geometry. At the BCP, the density is $\rho(\mathbf{r}_{BCP}) = 1.90$ e/Å^3, and the Laplacian assumes $\nabla^2\rho(\mathbf{r}_{BCP}) = 8.26$ e/Å^5. The sulfur center is at −0.52 Å, and the nitrogen center is at 0.92 Å.

TABLE 5: Influence of the Substituents on the Bond Topological Properties at the BCP of the S═N Bond of 4[a]

	d	ρ	$\nabla^2\rho$	λ_1	λ_2	λ_3	ϵ	d(N)	d(S)	d(N)/d(S)
R = H										
6-31G(d,p)	1.53	1.85	6.29	−10.96	−7.08	24.34	0.55	0.94	0.95	1.58
6-311G(d,p)	1.53	1.89	3.54	−11.32	−7.50	22.37	0.51	0.93	0.60	1.56
R = Me										
6-31G(d,p)	1.54	1.83	5.44	−10.57	−6.78	22.79	0.56	0.94	0.60	1.58
6-311G(d,p)	1.53	1.86	3.67	−10.91	−7.16	21.74	0.52	0.93	0.60	1.56
R = *t*Bu										
6-31G(d,p)	1.54	1.81	5.32	−10.33	−6.74	22.40	0.53	0.94	0.60	1.57
6-311G(d,p)	1.53	1.84	3.95	−10.61	−7.06	21.62	0.50	0.93	0.60	1.55

[a] The geometry was optimized on the indicated level of theory. Distances are given in Å, densities are given in e/Å^3, and second derivatives are given in e/Å^5.

behavior of the (2d,p) set. For the 6-31G(2d,p) and 6-311G-(2d,p) basis sets, the [d(N)/d(S)] values are somewhat smaller than for the basis sets with 1d or 3d polarization functions. For formal single bonds, the variations of the λ_i values along the bond path are similar, but the BCP is located close to the middle of the bonds. In this region, λ_3 also changes slowly. As a consequence, its dependency on the method of calculation is considerably weaker.

The strong deviations between experiment and theory could be caused by the fact that the sterically demanding substituents employed in the experimental studies are quite often replaced by smaller groups. Sterically demanding substituents mainly change the kinetic stability, while the electronic structure is less influenced. Consequently, for less sensitive properties, such a replacement is surely justified. For more sensitive properties such as the Laplacian at the BCP of polar bonds, one needs to test whether this simplification within theory does not influence such properties too much. For the present model systems, we find only a weak dependency of the bond topological properties, as shown in Table 5 for the formal SN double bonds of S(NR)$_3$, R = H, Me, *t*Bu, which were selected as examples, because the formal double bonds show a strong sensitivity of λ_3, in particular. Similar variations were obtained for all other compounds. Employing the 6-311G(d,p) basis set, the Laplacian varies in the series R = H, Me, *t*Bu from 3.54 to 3.95 e/Å^5. This change is smaller than the variations obtained

TABLE 6: Influence of the Theoretical Approach on the QTAIM Charges of 4; R = Me[a]

	Q(S)	*Q*(N)	$Q(N_\Sigma)$[b]
HF/6-311G(d,p))	+3.65	−1.78	−1.22
MP2/6-31G(d,p)	+3.27	−1.64	−1.10
B3PW91/6-31G(d,p)	+2.85	−1.4	−0.95
B3LYP/6-311G(d,p)	+2.71	−1.32	−0.90
B3PW91/6-311G(d,p)	+2.77	−1.36	−0.92

[a] Geometries have been optimized at the indicated level of theory. Charges are given in e. [b] The $\sum$ denotes the summation of the atomic charges of the nitrogen atom and the substituent.

TABLE 7: Bond Orders of $S(NCH_3)_2$, 3, According to Cioslowski[a]

	S1−N2	S1−N1	N2−N1	N2−C2	N1−C1
		B3PW91			
6-311G(d,p)	1.78	1.72	0.32	0.99	0.99
6-311G(2d,p)	1.83	1.77	0.28	1.01	1.01
6-311G(3d,p)	1.78	1.73	0.29	1.00	1.00
6-31G(d)	1.76	1.70	0.33	0.99	0.99
6-31G(d,p)	1.76	1.70	0.33	0.98	0.98
6-31G(2d,p)	1.82	1.77	0.29	1.00	1.00
6-31G(3d,p)	1.77	1.72	0.30	0.99	0.99
cc-pVDZ	1.76	1.71	0.32	0.98	0.97
		B3LYP			
6-311G(d,p)	1.79	1.73	0.32	0.99	0.98
		MP2			
6-31G(d)	1.64	1.64	0.29	0.93	0.93
6-31G(2d,p)	1.71	1.69	0.25	0.94	0.93

[a] Geometry was optimized at the indicated level of theory.

if the basis set is enlarged from 6-31G(d,p) to the 6-311G(d,p) basis set. The ratio [*d*(N)/*d*(S)] remains nearly unaffected also if the substituents are changed. Thus, within the present series of model compounds for comparing bond topological properties between experiment and theory, it seems reasonable to make calculations for the molecules with the smaller substituents R = Me instead of R = *t*Bu; even R = H is a good approximation.

Within the Bader approach, the atomic charges are obtained by integrating the charge density over the atomic basins. With compound **4** as a typical example, Table 6 summarizes the variations in the computed atomic charges as a function of some methods of calculation and basis sets. Hartree−Fock predicts the highest charges, which is expected, because it tends to overestimate the ionicity of bonds. A considerable difference is also found between the MP2 approach and DFT, and a more flexible basis set also seems to be of importance. Our attempt to test even larger basis sets failed because of problems establishing the strongly curved zero-flux surfaces around the sulfur centers.

Quite often, the bond strength is discussed in terms of the bond order. In the present study, the bond orders according to Cioslowski[50] were calculated. They are a measure of the purely covalent character of the bond. We used compound **3**, R = Me, to investigate the variations in the computed values on the theoretical approach. Table 7 shows the calculated values for the two SN formal double bonds and the two NC formal single bonds as a function of some theoretical approaches and basis set sizes. Additionally, an NN bond order is given. Comparing the bond order variations to those found for the computed topological properties, we found the bond order to be quite insensitive. This holds true particularly for the bond orders of the formal NC single bonds, for which all DFT values are between 0.99 and 1.01 and the MP2 results deviate only slightly, and also for formal double bonds for which the Laplacian values and atomic charges varied considerably. The S1═N2 bond orders predicted by DFT are between 1.76 and 1.83. If, as suggested by the analysis of the Laplacian, the (2d,p) set is regarded as an outlier, the variations are only 1−2%. The MP2 approach deviates from the DFT results by about 5%. Although the topological analysis of this molecule yields no bond path between the nitrogen atoms, a bond order of roughly 0.30 is calculated. The B3LYP value differs only 0.01 unit from the corresponding B3PW91 values, while the MP2 values are again somewhat smaller.

Up to now, all topological properties were computed for optimized geometries. To ensure that the variations discussed already do not mainly result from small changes in the computed bond distances, we repeated some of the calculations at experimental geometries. These results are summarized in Table 8, which shows that the variations in ρ and $\nabla^2\rho$ remain (i.e. the small changes in the bond distances found in the former cases cannot be mainly responsible for the high sensitivity discussed here). Because experimental geometries were used in combination with the substituents employed in the experiment, Table 8 provides a direct comparison between theoretical and experimental values for the formal SN double bonds, which seem to be the most difficult to describe. Therefore, Table 8 also gives the experimental values.[36] It is obvious that all experimental values at the BCP lie outside the range spanned by theory. Most obvious are the different positions of both BCPs which were already discussed in combination with the formal double bond S1═N2 of compound **1a** (Table 1). Although the experimental BCP is located almost in the middle of the bond, [*d*(N)/*d*(S)] $\approx$ 1, theory predicts it to be much closer to the sulfur center, [*d*(N)/*d*(S)] $\approx$ 1.5. To investigate this disagreement, we computed the values at the experimental position of the BCP, which are given in the last row. This was already suggested by ref 25, in which a better agreement was obtained between theory

TABLE 8: Bond Topological Properties at the BCP of the Formal S═N Double Bond of 4 with R = *t*Bu [$S(NtBu)_3$] Computed at the Experimental Geometry[a]

	ρ	$\nabla^2\rho$	λ_1	λ_2	λ_3	ϵ	*d*(N)	*d*(S)	*d*(N)/*d*(S)
STO-3G	1.49	21.67	−5.83	−3.53	31.04	0.65	0.93	0.59	1.58
SV	1.69	5.75	−7.86	−6.52	20.13	0.21	0.90	0.61	1.47
6-31G(d,p)	1.88	10.61	−11.00	−7.30	28.92	0.51	0.92	0.59	1.57
6-311G(d,p)	1.90	8.09	−11.15	−7.51	26.75	0.49	0.92	0.59	1.56
6-311G(2d,p)	1.94	−7.45	−12.09	−8.20	12.84	0.47	0.89	0.62	1.43
6-311G(3d,p)	1.93	−1.06	−12.09	−8.18	19.21	0.48	0.90	0.61	1.47
6-311++G(d,p)	1.90	8.64	−11.76	−7.54	27.36	0.56	0.92	0.59	1.57
				Experimental					
	2.27	−10.56	−14.40	−11.83	15.69	0.22	0.78	0.74	1.05
6-311++G(d,p)[b]	1.95	−14.28	−11.26	−7.64	4.48	0.47	0.78	0.74	1.05

[a] Distances are given in Å, densities are given in e/Å^3, and second derivatives are given in *e*/Å^5. [b] Bond topological values at the position of the experimental BCP.

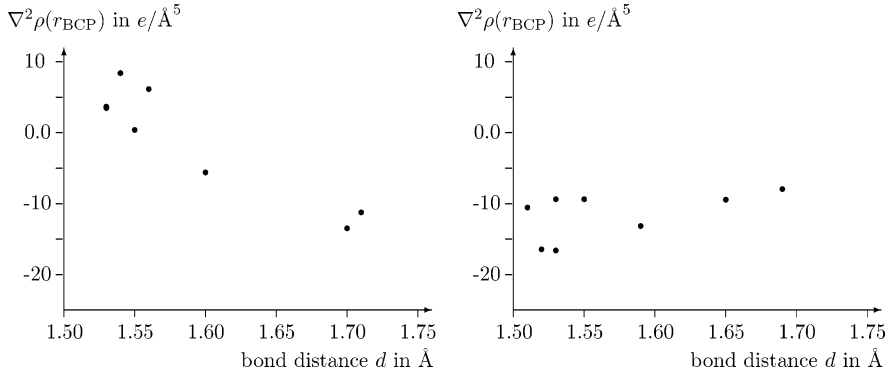

Figure 3. Correlation between bond distance d and Laplacian $\nabla^2\rho(\mathbf{r}_{BCP})$ for all SN bonds. Left: Optimized methyl-substituted model compounds **1**−**4**, calculated at the B3PW91/6-311G(d,p) level of theory. Best linear fit: $\nabla^2\rho(\mathbf{r}_{BCP}) = -91.11d + 154.53$, $R^2 = 0.890$. Right: Experimental values. Best linear fit: $\nabla^2\rho(\mathbf{r}_{BCP}) = 11.16d - 29.83$, $R^2 = 0.053$.

TABLE 9: Comparison between the Experimental and Theoretical Densities in e/Å^3 at the Sulfur and Nitrogen Nuclei

	experiment				theory			
compound	S1	N1	N2	N3	S1	N1	N2	N3
1b	17 974	1391	1392		17 462	1310	1313	
2a	17 996	1391	1391	1392	17 455	1310	1311	1312
3	17 981	1391	1390		17 464	1313	1314	
4	18 025	1395			17 455	1313		

and experiment. However, for the present compounds, it does not improve the agreement. The deviation in the density remains, and abetter agreement in the Laplacian results from compensation between λ_2 and λ_3. Both individual values deviate more if the theoretical values taken at the position of the experimental BCP are compared with the experimental results.

Table 8 shows that at the theoretical and experimental positions of the BCPs the computed density is smaller than its experimental counterpart, indicating that in the whole bonding region the computed density is considerably smaller than the experimental one. It is interesting to note that a similar behavior is also found at the position of the nuclei, as shown in Table 9.

A direct comparison needs, at least, a correlation of the corresponding experimental and theoretical values. For the given set of model compounds, such a relationship exists for the densities (see Figure 2 of ref 36). In ref 36, we showed that both the theoretically and experimentally determined densities at the BCPs correlate with the bond distances. Figure 3 shows a similar correlation between the Laplacians at the BCPs and the bond distances exclusively for the theoretical description. Table 10 summarizes the results of the linear regressions for the Laplacians versus bond distances and also repeats the results obtained for the correlation of the densities with bond distances. The missing correlation between the experimental Laplacian and the bond distances is obvious.

Table 10 also offers information on the extent to which experimentally determined geometries can be employed in a theoretical determination of densities and Laplacians. If the bond topological properties are computed from single point calculations at the experimental equilibrium geometries with medium to large basis sets, the bond distances correlate with the densities and Laplacians at the BCP. If smaller basis sets are employed, only a correlation between bond distances and densities at the BCP exists; the correlation between bond distances and Laplacians is no longer found. For theoretically optimized equilibrium geometries, the correlation also exists in this case. The destruction of the correlation between the Laplacian values at the BCPs and bond distances found for the smaller basis sets in combination with the experimental geometries occurs, because such basis sets tend to overestimate the bond distances of the single bonds considerably. As compared to the respective equilibrium geometry of the given approach, the theory describes compressed bonds if the experimental geometries are employed. From this point of view, computations which employ theoretically optimized geometries seem to be favorable with respect to those which use the experimental geometries. If experimental geometries are used, they have to be combined with very flexible basis sets. It is also obvious that, as a consequence of the different correlations with respect to the bond distances, both theoretically and experimentally determined Laplacians do not correlate with each other. Indeed, we find an R^2 value of 0.11. Consequently, a direct comparison is problematic.

The differences between the experimentally and theoretically determined Laplacian values are not only connected to the λ_3 values. Also, for the λ_1 and λ_2 Eigenvalues, no correlation can be expected, because the experimental and theoretical values of ϵ behave differently. Theoretical values obtained for the formal single and formal double bonds differ by approximately 0.3, while the experimental values are virtually identical. A similar situation is found for the BCPs. The theory predicts different positions for different formal types of SN bonds, but the experimentally determined positions remain nearly unchanged (compare, for example, Tables 1 and 2). Because, as discussed previously,[36] the SN formal single and double bonds

TABLE 10: Linear Regression on Theoretically and Experimentally Derived Bond Topological Properties at the BCP $\rho(\mathbf{r}_{BCP})$ and $\nabla^2\rho(\mathbf{r}_{BCP})$ vs Bond Distance d for Eight Different SN Bonds[a]

		$\rho = a\cdot d + b$			$\nabla^2\rho = a\cdot d + b$		
	calculation	a	b	R^2	a	b	R^2
experiment	sp[b]	−3.12	7.01	0.784	+11.16	−29.83	0.053
B3PW91/6-311G(d,p)	sp	−2.38	5.50	0.939	−28.37	45.35	0.046
B3PW91/6-311G(d,p)	opt[b]	−2.22	5.25	0.967	−91.11	154.53	0.890
B3PW91/6-311++G(d,p)	sp	−2.24	5.19	0.694	−91.89	144.58	0.633

[a] The linear regression implies no model building. [b] Single point (sp) calculations were done at the experimental (solid state) geometry, R = *t*Bu. [c] The optimization was performed employing the methyl-substututed compounds.

TABLE 11: Leading Natural Lewis Structures Obtained from the NBO/NRT Analysis[a]

Ls 1	Ls 2	Ls 3
compound **1b**		
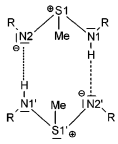	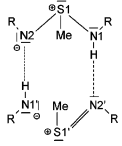	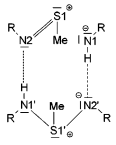
compound **2b**		
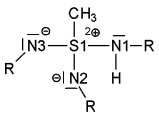	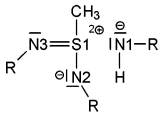	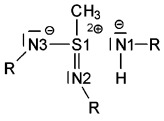
compound **4**		
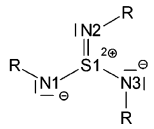	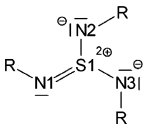	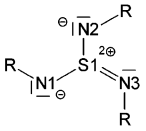

[a]Optimized geometries were used.

are quite different in nature (considerably higher ionic character of the formal double bonds), variations in the density-related properties, as predicted by theory, seem to be reasonable.

The discussion shows that, on the experimental side only, the less sensitive properties at the BCP (e.g., density) reveal a correlation with bond distance or with the formal type of bond. For the more sensitive parameters (e.g., second derivatives and related quantities), no correlation is found. Despite the dependency on the method of calculation for the theoretically determined data, the corresponding correlations are found for all properties. From the present study, one cannot answer why the experimental data do not show the expected correlation . This could arise from uncertainties which enter the experimental data during the refining process as was shown by recent investigations.[29−31] For the nonpolar CC bonds of C_{60} derivatives, Wagner et al. found all correlations discussed here.[34]

B. Investigation of Dependency of NBO/NRT Properties on the Method. In a previous paper,[36] QTAIM and NBO/NRT approaches complemented each other in the investigation of the bonding properties of the present set of model compounds. The application of the topological QTAIM analysis enables the comparison of the qualitative features of the experimentally and theoretically determined density distributions. The NBO/NRT approach allows the detection of more subtle details of the bonding character. They were also present within the QTAIM parameter; however, because of the strong dependencies discussed already, a support was necessary to avoid an overinterpretation. Because some authors claim a strong dependency on the method of computations for the NBO/NRT results,[50] we investigated the dependencies of data obtained from the NBO/NRT approach on the theoretical approach. The results are summarized in Tables 11-16. As for QTAIM investigations, we chose some typical bonds to illustrate the overall behavior. In Table 11, the leading Lewis structures are depicted, which will be denoted as Ls 1 to Ls 3. Tables 12−16 summarize the variations in weights and in the computed total, covalent, and ionic bond orders (BOt, BOc, BOi, respectively[69−71]). Finally, the atomic charges, *Q*'s, also obtained from the NBO analyses, are given. *Q*(X) denotes the atomic charge of atom X. When atom X is connected to a substituent R = H, Me or R = *t*Bu, then the summed up atomic charges are also given and denoted as $Q(X_\Sigma) = Q(X) + Q(H)$, $Q(X_\Sigma) = Q(X) + Q(Me)$, and $Q(X_\Sigma) = Q(X) + Q(t\text{Bu})$, respectively.

TABLE 12: Influence of the Theoretical Approach on the NBO/NRT Expansion and on the Computed Bond Orders of 1b (R = Me)[a]

	MP2[c]	B3LYP	B3PW91
Ls 1[b]	56.2%	38.8%	38.0%
Ls 2	5.1	9.2	8.1
Ls 3	5.1	9.2	7.5
		S1−N1	
BOt	0.95	0.92	0.92
BOc	0.68	0.67	0.67
BOi	0.27	0.25	0.25
		S1═N2	
BOt	1.05	1.10	1.09
BOc	0.81	0.82	0.81
BOi	0.24	0.28	0.28
		S1−C	
BOt	0.97	0.96	0.96
BOc	0.90	0.90	0.90
BOi	0.07	0.06	0.06
		N2···H	
BOt	0.01	0.02	0.02
BOc	0.00	0.00	0.00
BOi	0.01	0.02	0.02

[a] The corresponding Lewis structures can be taken from Table 11. [b] The geometries were optimized with the 6-31G(d,p) basis set and the indicated method. The initial three lines give the respective weights of the leading resonance structures. The other lines give the total (BOt), covalent (BOc), and ionic (BOi) bond orders for different bonds as obtained from the NRT analysis. [c] This calculation was done by imposing inversion symmetry.

TABLE 13: Influence of the Basis Set Size on the NBO/NRT Expansion and the Computed Bond Orders of 2b (R = Me) Obtained from the NRT Analysis[a]

	6-31G(d,p)	6-311G(d,p)	6-31G(3d,p)	cc-pVDZ	cc-pVTZ
Ls 1[b]	33.97%	33.24%	27.20%	33.49%	41.12%
Ls 2	12.91	13.18	13.36	15.20	3.90
Ls 3	10.95	10.16	12.86	9.65	15.93
			S1−N1		
BOt	0.58	0.57	0.54	0.56	0.70
BOc	0.36	0.39	0.34	0.37	0.45
BOi	0.22	0.18	0.20	0.19	0.25
			S1═N2		
BOt	1.18	1.16	1.17	1.17	1.25
BOc	0.81	0.85	0.78	0.84	0.86
BOi	0.36	0.32	0.39	0.33	0.39
			S1═N3		
BOt	1.24	1.23	1.26	1.24	1.11
BOc	0.86	0.89	0.83	0.88	0.81
BOi	0.39	0.33	0.43	0.36	0.30
			S1−C7		
BOt	0.89	0.90	0.89	0.90	0.89
BOc	0.85	0.89	0.83	0.88	0.85
BOi	0.04	0.01	0.07	0.02	0.04

[a] The corresponding Lewis structures can be taken from Table 11. [b] The geometry optimizations were performed employing the B3PW91 functional and the indicated basis set. The initial three lines give the respective weights of the leading resonance structures. The other lines give the total (BOt), covalent (BOc), and ionic (BOi) bond orders for different bonds as obtained from the NRT analysis.

The tables show that the weights of the leading Lewis structures depend considerably upon the theoretical approach, as well as on the size of the AO basis sets. For compound **1b**, for example, the weight of Ls 1 drops from about 56% to about 38% if we compare the MP2 result with the B3PW91 data (Table 12). If the hydrogen or the methyl substituents are replaced by the bulky *t*Bu groups, which were used in the

TABLE 14: Influence of the Basis Set Size on the Atomic Charges of 2b in e, Predicted by the NBO Analysis

	6-31G(d,p)	6-311G(d,p)	6-31G(3d,p)	cc-pVDZ	cc-pVTZ
Q(S1)[a]	+2.03	+1.94	+2.09	+1.93	+1.98
Q(N1)	−0.94	−0.88	−0.96	−0.91	−0.87
Q(N1$_\Sigma$)[b]	−0.33	−0.31	−0.33	−0.31	−0.31
Q(N2)	−0.97	−0.94	−1.00	−0.95	−0.94
Q(N2$_\Sigma$)	−0.81	−0.79	−0.83	−0.78	−0.80
Q(N3)	−0.95	−0.93	−0.98	−0.95	−0.92
Q(N3$_\Sigma$)	−0.79	−0.77	−0.81	−0.77	−0.78
Q(C7)	−0.94	−0.78	−0.96	−0.84	−0.81
Q(C7$_\Sigma$)	−0.11	−0.07	−0.12	−0.06	−0.10

[a] The geometry optimizations were performed employing the B3PW91 functional and the indicated basis set. [b] The Σ denotes the summation of the atomic charges of the respective atoms and the substituents.

TABLE 15: Influence of the Substituents on the NBO/NRT Expansion on the Computed Bond Orders (BOs) and on Charges (Q's) in e of 4[a]

	R = H[a]	R = Me[a]	R = *t*Bu[a]
Ls 1−3	29.09%	25.12%	15.51%
	S═N Bond Order		
BOt	1.33	1.32	1.31
BOc	0.96	0.97	0.95
BOi	0.37	0.35	0.36
	Charge		
Q(S)	+1.88	+1.90	+1.96
Q(N)	−1.01	−0.84	−0.89
Q(N$_\Sigma$)[b]	−0.63	−0.63	−0.65

[a] The corresponding Lewis structures can be taken from Table 11. [b] The geometries have been optimized at the indicated level of theory. [c] The Σ denotes the summation of the charges of the substituents into the atomic charge.

TABLE 16: Influence of the Theoretical Approach on the NBO Charges in e of 4; R = Me

	Q(S)	Q(N)	Q(N$_\Sigma$)[a]
HF/6-311G(d,p)[b]	+2.23	−0.97	−0.74
MP2/6-31G(d,p)	+1.91	−0.84	−0.64
B3LYP/6-311G(d,p)	+1.90	−0.84	−0.63
B3PW91/6-311G(d,p)	+1.90	−0.84	−0.63
B3PW91/6-31G(d,p)	+1.96	−0.86	−0.65

[a] The geometry was optimized with the B3PW91 functional in combination with the 6-311G(d,p) basis set. [b] The Σ denotes the summation of the atomic charges of the respective atoms and the substituents.

experiment, the weights of the leading Lewis structures drop from around 30% to only 15% (Table 15). However, despite these strong variations, the computed bond orders and atomic charges remain almost constant. One example is the decreasing weights of the leading Lewis structures found for R = H compared to R = *t*Bu. The corresponding bond orders differ by only 1−2%. Similar changes are found if the basis set size or the method of computation is varied. The atomic charges vary to a somewhat larger extent, but, for this quantity also, the changes are less than 10%. If we compare Table 6 with Table 16, it is obvious that the atomic charges derived with the NBO/NRT approach are less sensitive with respect to the method of calculation than its QTAIM counterparts. The NBO-derived charges of the sulfur atoms mimic their formal oxidation state, as can be seen from Table 17.

C. Comparison of the QTAIM and NBO/NRT Approaches. As discussed already, in a previous paper, we combined the QTAIM and NBO/NRT approaches to investigate the nature of the SN bonds within our set of model compounds. This requires that the quantities obtained from both approaches correlate with each other. The comparison of the QTAIM- and NBO/NRT-derived atomic charges of the sulfur and nitrogen centers in all eight different SN bonds is given in Table 17. The linear regression of this data set yields $Q_{QTAIM} = 1.34Q_{NBO} + 0.09$ with a correlation coefficient of $R^2 = 0.99$, showing that both approaches predict similar trends. The slope of 1.34 in combination with an intercept of 0.09 reveals, however, that QTAIM charges are higher, which was also found in other studies (e.g., ref 67). The absolute values of both approaches agree for some centers but disagree for others. Table 17 shows that a nearly perfect agreement is found for the N1 center of **1a** and the N1 center of **2b** which form single bonds to three different neighbors. For all other nitrogen centers which form one bond to the sulfur atom and one to a carbon center, the deviation lies between 0.2 and 0.4 electron units. The differences found for the sulfur are also quite interesting. For **1a**,[72] which possesses only one dominant Lewis structure, a difference of only 0.19 electron units is found. For compound **4**, for which three equally contributing Lewis structures exist, the largest deviation of about 1 electron unit is obtained (i.e., the difference seems to correlate with the number of Lewis structures in the NBO/NRT approach possessing a weight higher than 0.2).

TABLE 17: Comparison of QTAIM and NBO Charges in e[a]

compound	center	Q(NBO)	Q(QTAIM)	$\Delta[\lvert Q(\text{QTAIM})\rvert - \lvert Q(\text{NBO})\rvert]$
1a	S1	1.13	1.32	0.19
1a	N1	−1.02	−1.07	0.05
1a	N2	−1.09	−1.32	0.23
2b	S1	1.89	2.42	0.53
2b	N1	−1.05	−1.07	0.02
2b	N2	−1.13	−1.44	0.31
2b	N3	−1.12	−1.46	0.34
3	S1	1.13	1.83	0.70
3	N1	−0.93	−1.29	0.36
3	N2	−0.91	−1.3	0.39
4	S1	1.88	2.86	0.98
4	N1	−1.01	−1.36	0.35

[a] All calculations were performed with the B3PW91 functional in combination with a 6-311G(d,p) basis set (R = H).

If the total bond orders computed within the NBO/NRT approach are compared to those obtained with the Cioslowski approach,[50] we find a linear regression of $BO_{QTAIM} = 0.96BO_{NBO} + 0.27$, $R^2 = 0.91$ (i.e., a slope of about 1 is found), but the Cioslowski approach always give a somewhat higher bond order. The difference is even larger if it is taken into account that according to Cioslowski[50] only the covalent bond order is computed, while the total bond order of the NBO/NRT approach is used. If ionic contributions, which are expected from the high atomic charges, were added to the Cioslowski bond order, the corresponding total bond orders become quite high.

However, although the QTAIM and the NBO/NRT approaches disagree in the actual numbers for bond orders and atomic charges, the trends for the series of compounds **1**−**4** are in line with each other. Both approaches predict increasing covalent as well as ionic contributions when comparing a formal single bond to a formal double bond. For the formal single S1−N1 bond of **2b** (R = Me, Table 13), NBO/NRT predicts a covalent bond order of 0.3−0.4 and an ionic contribution of approximately 0.2. For the formal double bonds S1═N2 and S1═N3 of the same molecule, covalent bond orders of approximately 0.8 are computed, and the ionic contribution is predicted to be 0.3−0.4. The bond order according to Cioslowski increases from 1.01 to 1.34 (for R = H, see Table 18), and as can be seen from Table 17, the absolute value of the atomic charge also increases from 1.07 for the N1 center to about 1.44

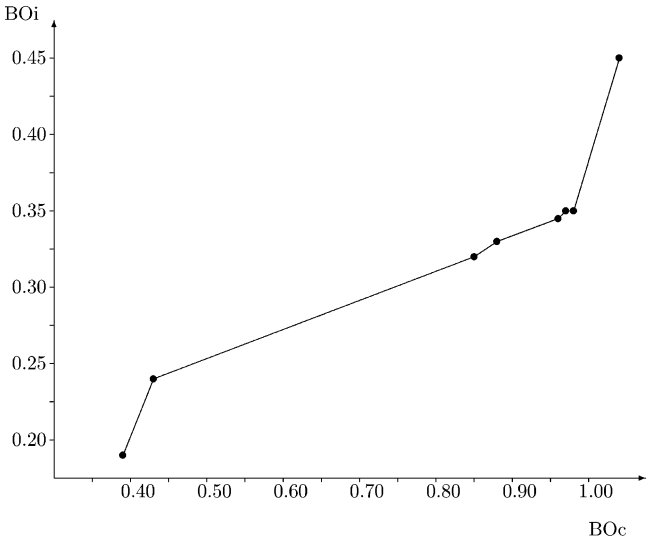

Figure 4. Ionic (BOi) versus covalent (BOc) NBO bond order in the eight different N−S bonds of **1b**, **2b**, **3**, and **4** (R = Me), calculated at the B3PW91/6-311G(d,p) level of theory (optimized geometries).

TABLE 18: Comparison of Cioslowski (CIO) and NBO Bond Orders[a]

compound	bond	NBO	CIO	Δ
1a	S1−N2	0.63	1.10	0.47
1a	N1−N2	1.31	1.52	0.21
1a	S1−C2	0.95	1.03	0.08
2b	S1−N1	0.59	1.01	0.34
2b	S1−N2	1.11	1.34	0.23
2b	S1−N3	1.31	1.37	0.07
2b	S1−C7	0.90	0.99	0.09
3	S1−N1	1.49	1.78	0.29
3	S1−N2	1.36	1.77	0.41
3	N1−N1	0.15	0.34	0.19
4	S−N	1.32	1.55	0.23
4	N−N	0.00	0.25	0.25

[a] All calculations were performed with the B3PW91 functional in combination with a 6-311G(d,p) basis set (R = H).

for the N2 and N3 centers (i.e., also in this picture, the covalent and the ionic bond strength increase). Figure 4 shows the correlation for the NBO/NRT approach.

This trend is also reflected in the densities and Laplacians at the BCP. For the B3PW91/6-311G(d,p) approach, the formal single bonds (S1−N1 in **1b** and **2b**) possess densities at the BCP of 1.32 and 1.37 e/Å^3. They are associated with Laplacians of −8.58 and −9.98 e/Å^5, respectively, showing that SN formal single bonds are comparable in density and Laplacian at the BCP. All formal double bonds possess increased densities, indicating increased covalent bonding. Simultaneously, the Laplacian values at the BCP are shifted toward positive values, which within the QTAIM theory indicate higher ionic contributions (see Figure 3).

IV. Summary and Conclusions

In the present study, a set of sulfur−nitrogen compounds, which contain SN formal single and double bonds and include nitrogen atoms involved in inter- and intramolecular hydrogen bonds, is used to study the dependency of the bond topological QTAIM properties and of the NBO/NRT data on the method of computations. Additionally, the theoretical results are compared to each other and to their experimental counterparts.

For the SN formal double bonds, our investigations show a quite strong dependency of the λ_3 values, and as a consequence, the Laplacians at the BCP also vary with respect to the theoretical approach and the size of the AO basis sets. The other Hessian Eigenvalues, λ_1 and λ_2, change to a smaller extent, and the density itself varies only slightly. For all other bonds, the variations with respect to the theoretical approach are smaller. It is interesting to note that all data obtained with the (2d,p) polarization basis set proposed by Pople are found to deviate considerably from the corresponding values from (1d,p) and (3d,p) polarization basis sets.

The strong influence of the theoretical approach on the λ_3 values found for the formal double bonds mainly occurs, because it varies remarkably near the BCPs. As a consequence, small variations in the position of the BCP already lead to large changes in λ_3 and in the Laplacian. Because λ_1 and λ_2 and the density change slowly, a smaller dependency of these properties with respect to the theoretical description results. For all other bonds (e.g., formal single S−N and S−C bonds), the BCP is located close to the middle of the respective bond. In this region, λ_3 also varies slowly, so that smaller dependencies result. Despite these strong variations for the formal double bonds, the computed densities and Laplacians at the BCPs are found to show a nice correlation with the computed bond distances and formal characters of the bonds. Within the NBO/NRT approach, the weights of the leading Lewis structures are found to depend strongly on the method of computations and basis set size; however, the derived properties such as bond orders and atomic charges are found to be almost independent.

Within our set of model compounds, the Cioslowski bond orders are considerably higher than the covalent bond orders in the NBO/NRT approach, and also, higher atomic charges are obtained in QTAIM theory than in the NBO approach. However, although both approaches disagree considerably in the actual numbers, they agree in the trends. Both predict increasing ionic and covalent bond contributions when comparing the SN formal single to the formal double bonds.

For the present set of model compounds, theory and experiment agree qualitatively in the topological features of the electron density, but both disagree in the absolute values of the density and the Laplacians at the BCPs. Already the positions of the BCPs are quite different. To study whether both can be directly compared, we studied the correlations between experimentally and theoretically derived quantities obtained for our set of eight different SN bonds. Such a correlation is only found for the less sensitive properties, such as density at the BCPs. The more sensitive ones (e.g., the Eigenvalues of the Hessian and the Laplacians) do not correlate. Comparing other relationships, we found that all theoretically derived properties correlate with bond distances or formal types of bonds; from the experimentally derived quantities, such relationships are only found for the density, while they are missing for the more sensitive properties. An example is the position of the BCP, which exclusively in the calculations clearly distinguishes formal single and double bonds. It is interesting to note that single point calculations of the density-related properties at experimentally derived geometries requires flexible basis sets. For smaller basis sets, the correlations between Laplacians and bond distances disappear. If both the geometries and density-related properties are obtained from theory, the correlations are also found for smaller basis sets.

From the present study, we cannot answer why a correlation between the Laplacians and bond distances is missing for the experimental data. In principle, it could turn out that the Hansen−Coppens formalism in its original form is not flexible enough to describe the topology (i.e., density and Laplacian at

the BCP) of the present SN bonds correctly. The little variation in the position of the experimental BCP supports this thesis. On the other side, there are examples of highly ionic bonding modes (e.g., in silicon compounds[68]) which show a BCP very close to the electropositive atom. The other possibility is that the Hansen−Coppens formalism is of sufficient flexibility, but multiple solutions exist in the least-squares refinement, maybe some of them of similar quality in the statistical quality measure. These questions are the matter of our future work.

Acknowledgment. This work was supported by the Deutsche Forschungsgemeinschaft within the framework of the Graduiertenkolleg 690: Elektronendichte: Theorie und Experiment.

References and Notes

(1) Bader, R. W. F. *Atoms in Molecules: A Quantum Theory*; Oxford University Press: Oxford, 1990.
(2) Coppens, P. *X-ray charge densities and chemical bonding*; Oxford University Press: Oxford, 1997; and references therein.
(3) Tsirelson, V. G.; Ozerov, R. P. *Electron Density and Bonding in Crystals*; IOP Publishing, Ltd: Bristol, 1996; and references therein.
(4) Koch, W.; Holthausen, M. C. *A Chemist's Guide to Density Functional Theory*; Wiley-VCH: Weinheim, 1999.
(5) Leach, A. R. *Molecular Modelling*; Dorset Press: Dorchester, 2001.
(6) Koritsansky, T. S.; Coppens, P. *Chem. Rev.* **2001**, *101*, 1583; and references therein.
(7) Parr, R. G.; Yang, W. *Density Functional Theory of Atoms and Molecules*; Clarendon Press: New York, 1989.
(8) Hohenberg, P.; Kohn, W. *Phys. Rev.* **1964**, *B136*, 864.
(9) Kohn, W.; Sham, L. J. *Phys. Rev.* **1965**, *A140*, 1133.
(10) Phillips, W.; Stanton, M.; O'Mara, D.; Li, Y.; Naday, I.; Westbrook, E. *Proc. SPIE-Int. Soc. Opt. Eng.* **1993**, *2003*, 133.
(11) Koritsanszky, T.; Flaig, R.; Zobel, D.; Krane, H.-G.; Morgenroth, W.; Luger, P. *Science* **1998**, *279*, 356.
(12) Volkov, A.; Wu, G.; Coppens, P. *J. Synchrotron Radiat.* **1999**, *6*, 1007.
(13) Kubicki, M.; Borowiak, T.; Dutkiewicz, G.; Souhassou, M.; Jelsch, C.; Lecomte, C. *J. Phys. Chem. B* **2002**, *106*, 3706.
(14) Hibbs, D. E.; Overgaard, J.; Platts, J. A.; Waller, M. P.; Hursthouse, M. B. *J. Phys. Chem. B* **2004**, *108*, 3663.
(15) Tsirelson, V.; Stash, A. *Chem. Phys. Lett.* **2002**, *351*, 142.
(16) Jayatilaka, D.; Grimwood, D. J. *Acta Crystallogr., Sect. A* **2001**, *57*, 76.
(17) Grimwood, D. J.; Jayatilaka, D. *Acta Crystallogr., Sect. A* **2001**, *57*, 87.
(18) Bytheway, I.; Grimwood, D. J.; Jayatilaka, D. *Acta Crystallogr., Sect. A* **2002**, *58*, 232.
(19) Bytheway, I.; Grimwood, D. J.; Figgis, B. N.; Chandler, G. S.; Jayatilaka, D. *Acta Crystallogr., Sect. A* **2002**, *58*, 244.
(20) Jelsch, C.; Teeter, M. M.; Lamzin, V.; Pichon-Pesme, V.; Blessing, R. H.; Lecomte, C. *Proc. Natl. Acad. Sci. U.S.A.* **2000**, *97*, 3171.
(21) Cachau, R.; Howard, E.; Barth, P.; Mitschler, A.; Chevrier, B.; Lamour, V.; Joachimiak, A.; Sanishville, R.; Van Zandt, M.; Sibley, E.; Moras, D.; Podjarny, A. *J. Phys. IV* **2000**, *10*, 3.
(22) Flaig, R.; Koritsanszky, T.; Dittrich, B.; Wagner, A.; Luger, P. *J. Am. Chem. Soc.* **2002**, *124*, 3407.
(23) Flaig, R.; Koritsanszky, T.; Janczak, J.; Krane, H.-G.; Morgenroth, W.; Luger, P. *Angew. Chem., Int. Ed.* **1999**, *38*, 1397.
(24) Li, X.; Wu, G.; Abramov, A.; Volkov, A. V.; Coppens, P. *Proc. Natl. Acad. Sci. U.S.A.* **2002**, *99*, 12132.
(25) Hibbs, D. E.; Austin-Woods, C. J.; Platts, J. A.; Overgaard, J.; Turner, P. *Chem.*−*Eur. J.* **2003**, *9*, 1075.
(26) Koritsansky, T. S.; Volkov, A. *Chem. Phys. Lett.* **2004**, *385*, 431.
(27) Flaig, R.; Koritsanszky, T.; Zobel, D.; Luger, P. *J. Am. Chem. Soc.* **1998**, *120*, 2227.
(28) Hansen, N. K.; Coppens, P. *Acta Crystallogr.* **1978**, *A34*, 909.
(29) Volkov, A.; Abramov, Y.; Coppens, P.; Gatti, C. *Acta Crystallogr., Sect. A* **2000**, *56*, 332.
(30) Volkov, A.; Coppens, P. *Acta Crystallogr., Sect. A* **2001**, *57*, 395.
(31) Koritsanszky, T.; Volkov, A.; Coppens, P. *Acta Crystallogr., Sect. A* **2001**, *58*, 464.
(32) Overgaard, J.; Waller, M. P.; Platts, J. A.; Hibbs, D. E. *J. Chem. Phys.* **2003**, *A107*, 11201.
(33) Arnold, W. D.; Sanders, L. K.; McMahon, M. T.; Volkov, V.; Wu, A. G.; Coppens, P.; Wilson, S. R.; Godbout, N.; Oldfield, E. *J. Am. Chem. Soc.* **2000**, *122*, 4708.
(34) Wagner, A.; Flaig, R.; Zobel, D.; Dittrich, B.; Bombicz, P.; Strümpel, M.; Luger, P. *J. Phys. Chem. A* **2002**, *106*, 6581.
(35) Tafipolsky, M.; Scherer, W.; Öfele, K.; Artus, G.; Pedersen, B.; Herrmann, W. A.; McGrady, G. S. *J. Am. Chem. Soc.* **2002**, *124*, 5865.
(36) Leusser, D.; Henn, J.; Kocher, N.; Engels, B.; Stalke, D. *J. Am. Chem. Soc.* **2004**, *126*, 1781.
(37) Peres, N.; Boukhris, A.; Souhassou, M.; Gaboille, G.; Lecomte, C. *Acta Crystallogr., Sect. A.* **1999**, *55*, 1038.
(38) Gatti, C.; Bianchi, R.; Destro, R.; Merati, F. *J. Mol. Struct.* **1992**, *255*, 409.
(39) Bianchi, R.; Gatti, C.; Adovasio, V.; Nardelli, M. *Acta Crystallogr., Sect. A* **1996**, *52*, 471.
(40) Gatti, C.; Saunders, R. V.; Roetti, C. *J. Chem. Phys.* **1994**, *101*, 10686.
(41) Gatti, C.; MacDougall, P. J.; Bader, R. F. W. *J. Chem. Phys.* **1988**, *88*, 3792.
(42) Byod, R. J.; Ugalde, J. M. In *Computational Chemistry: Structure, Interactions, and Reactivity*; Elsevier: Amsterdam, 1992; and references therein.
(43) Wang, J.; Shi, Z.; Boyd, R. J.; Gonzalez, C. A. *J. Phys. Chem.* **1994**, *98*, 6988; and references cited therein.
(44) Byod, R. J.; Wang, J.; Eriksson, L. A. In *Recent Advances in Density Functional Methods*; World Scientific Publishing: Singapore, 1995; and references.
(45) Cremer, D.; Kraka, E. *Croat. Chem. Acta* **1984**, *57*, 1259.
(46) Cheeseman, J. R.; Carroll, M. T.; Bader, R. F. W. *Chem. Phys. Lett.* **1988**, *143*, 450.
(47) Glendening, E. D.; Badenhoop, J. K.; Reed, A. E.; Carpenter, J. E.; Weinhold, F. *NBO 4.M*; Theoretical Chemistry Institute, University of Wisconsin: Madison, WI, 1999.
(48) Frisch, M. J.; Trucks, G. W.; Schlegel, H. B.; Scuseria, G. E.; Robb, M. A.; Cheeseman, J. R.; Zakrzewski, V. G.; Montgomery, J. A., Jr.; Stratmann, R. E.; Burant, J. C.; Dapprich, S.; Millam, J. M.; Daniels, A. D.; Kudin, K. N.; Strain, M. C.; Farkas, O.; Tomasi, J.; Barone, V.; Cossi, M.; Cammi, R.; Mennucci, B.; Pomelli, C.; Adamo, C.; Clifford, S.; Ochterski, J.; Petersson, G. A.; Ayala, P. Y.; Cui, Q.; Morokuma, K.; Malick, D. K.; Rabuck, A. D.; Raghavachari, K.; Foresman, J. B.; Cioslowski, J.; Ortiz, J. V.; Stefanov, B. B.; Liu, G.; Liashenko, A.; Piskorz, P.; Komaromi, I.; Gomperts, R.; Martin, R. L.; Fox, D. J.; Keith, T.; Al-Laham, M. A.; Peng, C. Y.; Nanayakkara, A.; Gonzalez, C.; Challacombe, M.; Gill, P. M. W.; Johnson, B. G.; Chen, W.; Wong, M. W.; Andres, J. L.; Head-Gordon, M.; Replogle, E. S.; Pople, J. A. *Gaussian 98*, revision A.7; Gaussian, Inc.: Pittsburgh, PA, 1998.
(49) Biegler König, F.; Schonebohm, J.; Bayels, D. *AIM2000* − A Program to Analyze and Visualize Atoms in Molecules. *J. Comput. Chem.* **2001**, *22*, 545.
(50) Cioslowski, J.; Mixon, T. *J. Am. Chem. Soc.* **1991**, *113*, 4142.
(51) Cheeseman, J. R.; Carroll, M. T.; Bader, R. W. F. *Chem. Phys. Lett.* **1988**, *143*, 450.
(52) Becke, A. D. *Phys. Rev.* **1988**, *A38*, 3098.
(53) Becke, A. D. *J. Chem. Phys.* **1993**, *98*, 5648.
(54) Perdew, J. P.; Wang, Y *Phys. Rev.* **1986**, *B33*, 8800.
(55) Lee, C.; Yang, W.; Parr, R. G. *Phys. Rev.* **1988**, *B37*, 785.
(56) Ditchfield, R.; Hehre, W. J.; Pople, J. A. *J. Chem. Phys.* **1971**, *54*, 724.
(57) Hehre, W. J.; Ditchfield, R.; Pople, J. A. *J. Chem. Phys.* **1972**, *56*, 2257.
(58) Hariharan, P. C.; Pople, J. A. *Mol. Phys.* **1974**, *27*, 209.
(59) Gordon, M. S. *Chem. Phys. Lett.* **1980**, *76*, 163.
(60) Hariharan, P. C.; Pople, J. A. *Theor. Chim. Acta* **1973**, *28*, 213.
(61) Woon, D. E.; Dunning, T. H., Jr. *J. Chem. Phys.* **1993**, *98*, 1358.
(62) Kendall, R. A.; Dunning, T. H., Jr., Harrison, R. J. *J. Chem. Phys.* **1992**, *96*, 6796.
(63) Dunning, T. H., Jr. *J. Chem. Phys.* **1989**, *90*, 1007.
(64) Peterson, K. A.; Woon, D. E.; Dunning, T. H., Jr. *J. Chem. Phys.* **1994**, *100*, 7410.
(65) Wilson, A.; van Mourik, T.; Dunning, T. H., Jr. *J. Mol. Struct.* **1997**, *388*, 339.
(66) Davidson, E. R. *Chem. Phys. Lett.* **1996**, *220*, 514.
(67) Meister, J.; Schwarz, W. H. E. *J. Phys. Chem.* **1994**, *98*, 8245.
(68) Kocher, N.; Henn, J.; Gostevskii, B.; Kost, D.; Kalikhman, I.; Engels, B.; Stalke, D. *J. Am. Chem. Soc.* **2004**, *126*, 5563.
(69) Glendening, E. D.; Weinhold, F. *J. Comput. Chem.* **1997**, *19*, 593.
(70) Glendening, E. D.; Weinhold, F. *J. Comput. Chem.* **1997**, *19*, 610.
(71) Glendening, E. D.; Badenhoop, J. K.; Weinhold, F. *J. Comput. Chem.* **1997**, *19*, 628.

(72) The two main Lewis structures for compound **1a** (see Figure 1) can be obtained from those of compounds **1b**, because **1b** is built up from two **1a** mnomers. The main Lewis structure of **1a** is obtained from Ls 1 of compound **1b** by omitting the upper monomer. The other, considerably less important structure is obtained from Ls 2 of **1b** by omitting the upper monomer. The third Lewis structure found for **1b** does not appear for **1a**. As can be seen from Table 12, only one dominant Lewis structure remains.